Suva

Chapter 5
Fiji Islands

The contributions of Alipate Waqaicelua, Varanisese Vuniyayawa, Ravind Kumar, Arieta Daphne and Bipendra Prakash from the Fiji Meteorological Service are gratefully acknowledged

Introduction

This chapter provides a brief description of the Fiji Islands, its past and present climate as well as projections for the future. The climate observation network and the availability of atmospheric and oceanic data records are outlined. The annual mean climate, seasonal cycles and the influences of large-scale climate features such as the South Pacific Convergence Zone and patterns of climate variability (e.g. the El Niño-Southern Oscillation) are analysed and discussed. Observed trends and analysis in air temperature, rainfall, extreme events including tropical cyclones, sea-surface temperature, ocean acidification and mean and extreme sea level are presented. Projections for air and sea-surface temperature, rainfall, sea level and ocean acidification for the 21st century are provided, as are projections for tropical cyclones, drought, extreme rainfall, and extreme temperature. These projections are presented along with confidence levels based on expert judgement by Pacific Climate Change Science Program (PCCSP) scientists. The chapter concludes with a summary table of projections (Table 5.4). Important background information, including an explanation of methods and models, is provided in Chapter 1. For definitions of other terms refer to the Glossary.

5.1 Climate Summary

5.1.1 Current Climate

- Changes in air temperature from season to season are relatively small and strongly tied to changes in the surrounding ocean temperature. The country has two distinct seasons – a warm wet season from November to April and a cooler dry season from May to October.
- The seasonal cycle is strongly affected by the South Pacific Convergence Zone, which is most intense during the wet season.
- The El Niño-Southern Oscillation is the most important influence on year-to-year climate variations.
- Annual and seasonal mean air temperatures at Suva and Nadi Airport have been increasing, particularly in the wet season over the period 1950–2009.
- Annual and seasonal rainfall trends for Suva and Nadi Airport for the period 1950–2009 are not statistically significant.
- The sea-level rise near Fiji measured by satellite altimeters since 1993 is about 6 mm per year.
- Tropical cyclones usually affect Fiji between November and April. Over the period 1969–2010, the centre of 70 tropical cyclones passed within 400 km of Suva. The high variability in tropical cyclone numbers makes it difficult to identify any long-term trends in frequency.

5.1.2 Future Climate

Over the course of the 21st century:

- Surface air temperature and sea-surface temperature are projected to continue to increase (*very high* confidence).
- Wet season rainfall is projected to increase (*moderate* confidence).
- Dry season rainfall is projected to decrease (*moderate* confidence).
- Little change is projected in annual mean rainfall (*low* confidence).
- The intensity and frequency of days of extreme heat are projected to increase (*very high* confidence).
- The intensity and frequency of days of extreme rainfall are projected to increase (*high* confidence).
- Little change is projected in the incidence of drought (*low* confidence).
- Tropical cyclone numbers are projected to decline in the south-east Pacific Ocean basin (0–40ºS, 170ºE–130ºW) (*moderate* confidence).
- Ocean acidification is projected to continue (*very high* confidence).
- Mean sea-level rise is projected to continue (*very high* confidence).

5.2 Country Description

Fiji is located in the western South Pacific Ocean between 177°E–178°W and 16°S–20°S. The country has 322 islands and a total land area of 18 333 km^2. The Exclusive Economic Zone has an area of 1.3 million km^2. The two largest islands are Viti Levu, 10 429 km^2, and Vanua Levu, 5 556 km^2. They take up 87% of the total land area and are mountainous and of volcanic origin with peaks up to 1 300 m. The other islands consist of small volcanic islands, low-lying atolls and elevated reefs (Fiji's First National Communication under the UNFCCC, 2005; Fiji's Pacific Adaptation to Climate Change, 2009). The estimated population of Fiji in 2010 was 844 420 (Fiji Country Statistics, SOPAC, 2010).

Viti Levu is the economic centre of Fiji, with Suva, the capital, located on the south coast, and Nadi, the tourism centre on the west coast.

Fiji's economy is based on sugar and tourism and over recent years the tourism sector has grown significantly. Most of the rural and urban population of Viti Levu live in the coastal zone where the majority of services, infrastructure, and economic activities are located (Fiji's First National Communication under the UNFCCC, 2005).

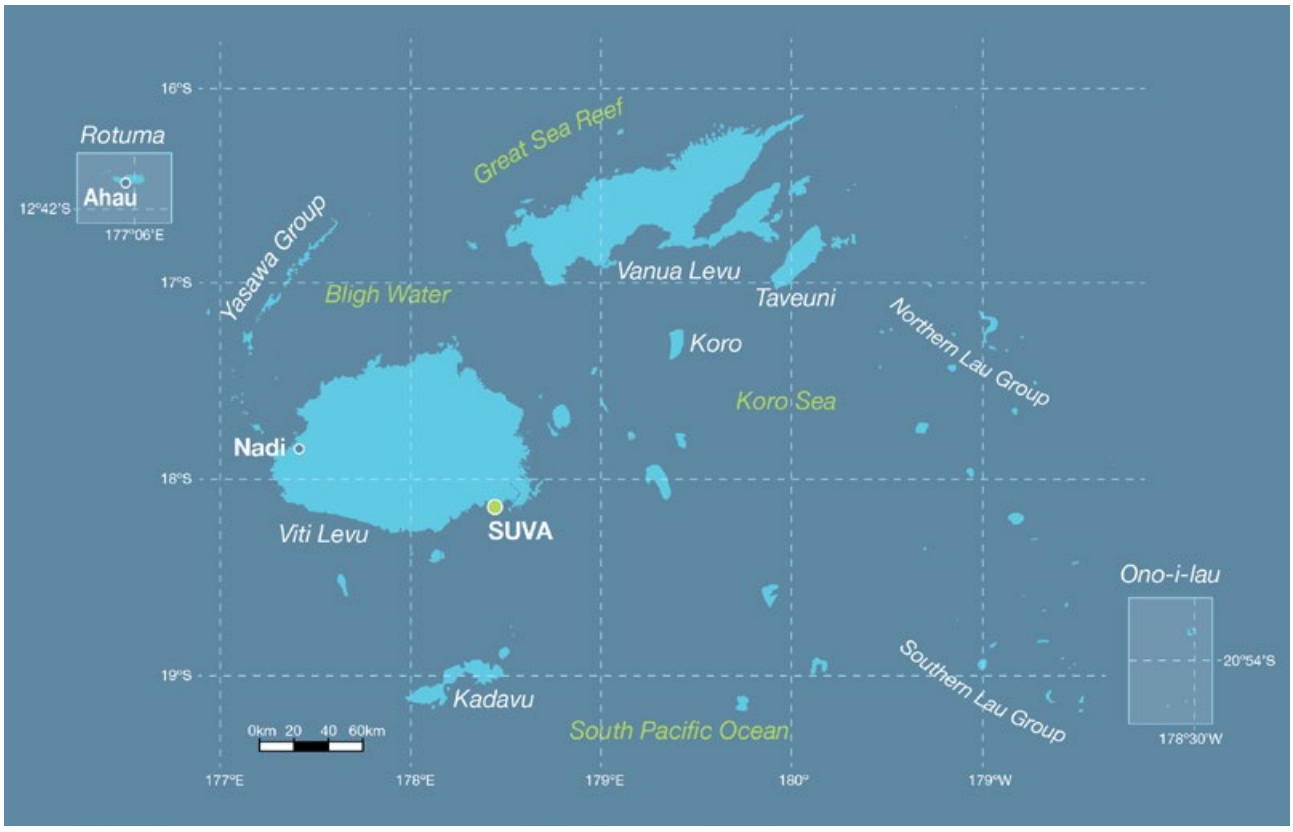

Figure 5.1: Fiji

5.3 Data Availability

There are currently 30 climate (single observation at 9 am), eight synoptic (multiple daily observations) and 52 rainfall-only operational meteorological observation stations in Fiji's meteorological network. Climate records with data available from before 1900 are available for at least six stations or multi-station composites.

Climate records for both Suva (the capital) and Nadi Airport from 1950–2009 have been used (Figure 5.1). Suva and Nadi Airport are located on the south-eastern and western sides of Viti Levu respectively. The records from both sites are homogeneous and more than 99% complete.

Oceanographic records do not cover such a long time period. Monthly-averaged sea-level data are available from Suva (1972–2009 and 1998–present) and Lautoka (1992–present). A global positioning system instrument to estimate vertical land motion was deployed at Lautoka in 2001 and will provide valuable direct estimates of local vertical land motion in future years. Both satellite (from 1993) and in situ sea-level data (1950–2009; termed reconstructed sea level; Volume 1, Section 2.2.2.2) are available on a global 1° x 1° grid.

Long-term locally-monitored sea-surface temperature data are unavailable for Fiji, so large-scale gridded sea-surface temperature datasets have been used (HadISST, HadSST2, ERSST and Kaplan Extended SST V2; Volume 1, Table 2.3).

Barometric pressure meter, Fiji Meteorological Service

5.4 Seasonal Cycles

Average monthly maximum, mean and minimum air temperatures are strongly tied to changes in the surrounding ocean temperature (Figure 5.2). The range in average monthly maximum temperature is about 4ºC for Suva and 3ºC for Nadi Airport. In the cooler/drier half of the year (May-October) less energy is received from the sun, south-east trade winds persist and sub-tropical high pressure systems move north bringing cooler, drier conditions. About 63% of Suva's rain and 77% of Nadi Airport's rain falls in the wet season from November to April.

The seasonal cycle is strongly affected by the South Pacific Convergence Zone (SPCZ), which is most intense during the wet season. The southern edge of the SPCZ usually lies near Fiji. The effects of large-scale climate features such as the SPCZ and trade winds are modified on some islands due to the influence of mountains. Those regions exposed to the trade winds can receive mean annual rainfall in excess of 4000 mm, while leeward regions receive on average less than 2000 mm annually with less than 25% of annual rainfall between May and October. Several weather features have a notable impact on Fiji's climate. Active phases of the Madden-Julian Oscillation (MJO; Volume 1, Section 2.4.4) near Fiji can be associated with significant rainfall for several days in the wet season. In addition, late afternoon convective thunderstorms contribute significant rainfall to the central and western parts of Viti Levu. In the dry season, cold fronts, which are usually weak by the time they reach Fiji's latitude, occasionally merge with troughs in the upper atmosphere resulting in widespread rainfall.

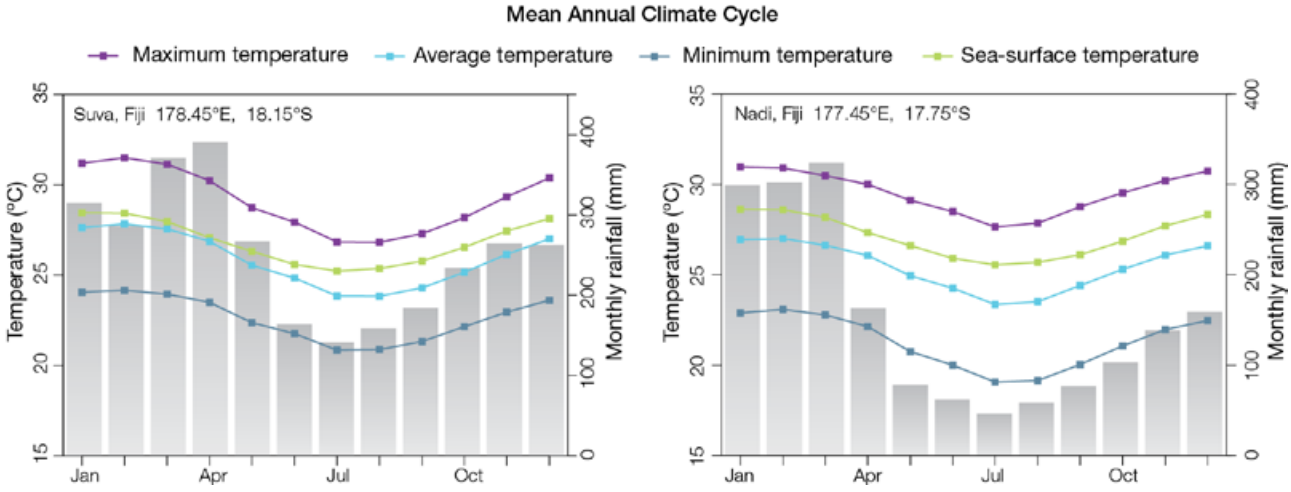

Figure 5.2: Mean annual cycle of rainfall (grey bars) and daily maximum, minimum and mean air temperatures at Suva (left) and at Nadi Airport (right), and local sea-surface temperatures derived from the HadISST dataset (Volume 1, Table 2.3).

5.5 Climate Variability

The El Niño-Southern Oscillation (ENSO) is the most important influence on year-to-year climate variations in Fiji. At Suva (Table 5.1), dry seasons during El Niño tend to be drier and cooler than normal, with the influence of ENSO much stronger on temperature than on rainfall. The opposite changes tend to occur during La Niña events (Figure 5.3). The influence is probably due to the cooler ocean waters around Fiji and more southerly and stronger trade winds (which are cooler and drier) in El Niño years. The Southern Annular Mode (SAM) is related to climate variability in the region, independent of but weaker than ENSO in the dry winter season. When the SAM index is positive, sub-tropical high pressure systems stay further south and temperatures are warmer, and when the SAM index is negative they move north, bringing cooler conditions. In the wet season only ENSO has a clear influence and only on temperature, with warmer nights and cooler days in El Niño years. Modoki El Niño events (Volume 1, Section 3.4.1) bring cooler days in the dry season and warmer nights in the wet season, as do classical El Niño events, but Modoki events have no significant influence on rainfall.

At Nadi Airport (Table 5.2) the dry season in El Niño years also tends to be cooler and drier. In the wet season the impact of ENSO is very strong. In El Niño years Nadi Airport wet seasons are drier (more than 50% of year-to-year rainfall variability can be explained by the central Pacific sea-surface temperature (Niño3.4) and days are warmer. Much of this variability is driven by the SPCZ, which moves to the north-east, away from Fiji, during El Niño events. This brings drier conditions to Nadi Airport, and with the decreased cloud cover this leads to warmer daytime temperatures. The opposite changes tend to occur in La Niña years. Modoki El Niño events have the same but weaker effects as canonical El Niño events in the wet season at Nadi Airport. SAM is correlated with only maximum temperatures at Nadi Airport but in the same way as in Suva.

The differences in climate between Suva and Nadi Airport are primarily due to their different exposure to the trade winds. Differences are greatest during the dry season when the trade winds dominate Fiji's weather. Suva's rainfall during the dry season is more than two and a half times that of Nadi Airport's. Wet season rainfall is similar, 1890 mm and 1385 mm respectively.

Table 5.1: Correlation coefficients between indices of key large-scale patterns of climate variability and minimum and maximum temperatures (Tmin and Tmax) and rainfall at Suva. Only correlation coefficients that are statistically significant at the 95% level are shown.

Climate feature/index		Dry season (May–October)			Wet season (November–April)		
		Tmin	Tmax	Rain	Tmin	Tmax	Rain
ENSO	Niño3.4	-0.53	-0.68	-0.36	0.47	-0.26	
	Southern Oscillation Index	0.45	0.69	0.31	-0.45	0.24	
Interdecadal Pacific Oscillation Index							
Southern Annular Mode Index		-0.33	-0.29				
ENSO Modoki Index			-0.41		0.37		
Number of years of data		68	67	68	68	68	68

Table 5.2: Correlation coefficients between indices of key large-scale patterns of climate variability and minimum and maximum temperatures (Tmin and Tmax) and rainfall at Nadi Airport. Only correlation coefficients that are statistically significant at the 95% level are shown.

Climate feature/index		Dry season (May–October)			Wet season (November–April)		
		Tmin	Tmax	Rain	Tmin	Tmax	Rain
ENSO	Niño3.4	-0.44	-0.57	-0.30		0.63	-0.73
	Southern Oscillation Index	0.33	0.50	0.30		-0.63	0.76
Interdecadal Pacific Oscillation Index							
Southern Annular Mode Index			-0.32			0.29	
ENSO Modoki Index			-0.25			0.37	-0.56
Number of years of data		65	65	67	65	66	66

5.6 Observed Trends

5.6.1 Air Temperature

Warming trends have been identified in annual and seasonal mean air temperatures at Suva and Nadi Airport for the period 1950–2009 (Figure 5.3). Annual and wet season maximum air temperature trends are greater than those observed for minimum air temperatures (Table 5.3) at both Suva and Nadi Airport.

5.6.2 Rainfall

Annual and seasonal rainfall trends for Suva and Nadi Airport for the period 1950–2009 are not statistically significant (Table 5.3 and Figure 5.4).

5.6.3 Extreme Events

The tropical cyclone season in Fiji is usually between November and April, but occasionally tropical cyclones have occurred in October and May in El Niño years. The tropical cyclone archive of the Southern Hemisphere indicates that between the 1969/70 and 2009/10 seasons, the centre of 70 tropical cyclones (Figure 5.5) passed within 400 km of Suva, usually approaching Fiji from the north-west. This represents an average of 17 cyclones per decade. Tropical cyclones were most frequent in El Niño years (19 cyclones per decade) and least frequent in La Niña years (15 cyclones per decade).

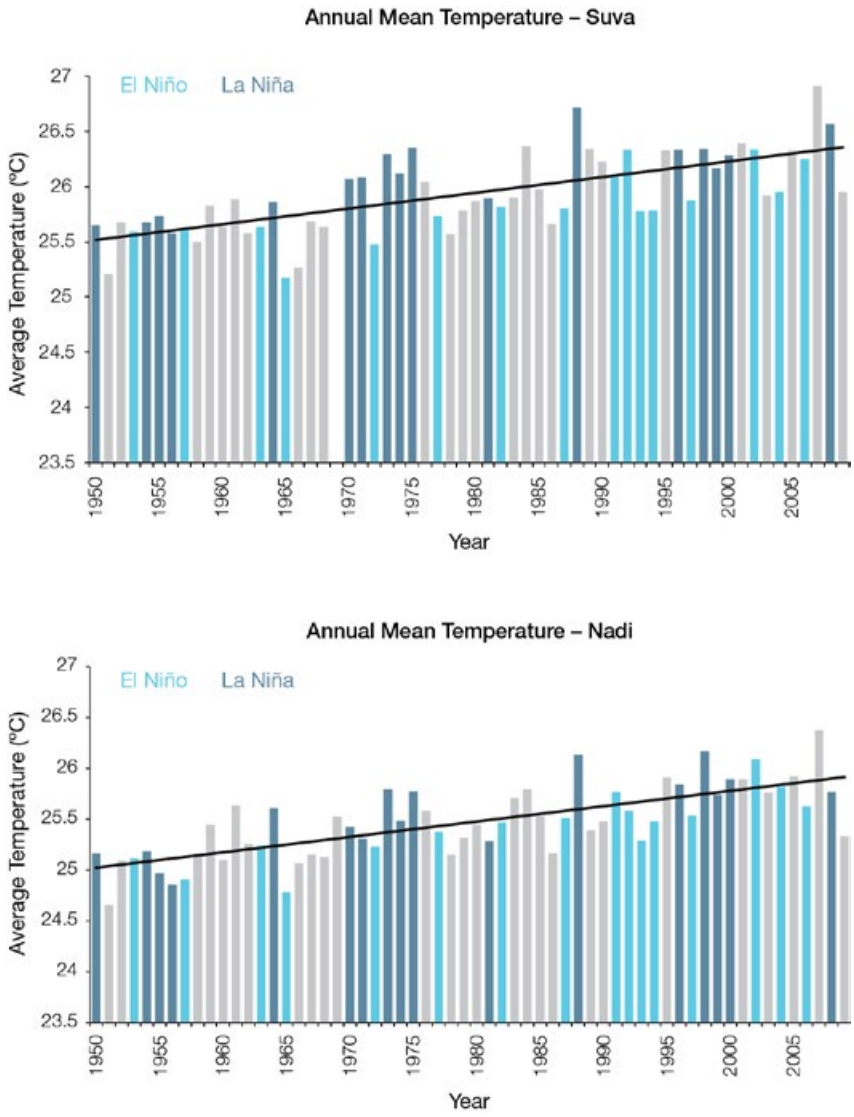

Figure 5.3: Annual mean air temperature for Suva (top) and Nadi Airport (bottom). Light blue, dark blue and grey bars denote El Niño, La Niña and neutral years respectively.

Table 5.3: Annual and seasonal trends in maximum, minimum and mean air temperature (Tmax, Tmin and Tmean) and rainfall at Suva and Nadi Airport for the period 1950–2009. Asterisks indicate significance at the 95% level. Persistence is taken into account in the assessment of significance as in Power and Kociuba (in press). The statistical significance of the air temperature trends is not assessed.

	Suva Tmax (°C per 10 yrs)	Suva Tmin (°C per 10 yrs)	Suva Tmean (°C per 10 yrs)	Suva Rain (mm per 10 yrs)	Nadi Airport Tmax (°C per 10 yrs)	Nadi Airport Tmin (°C per 10 yrs)	Nadi Airport Tmean (°C per 10 yrs)	Nadi Airport Rain (mm per 10 yrs)
Annual	+0.15	+0.14	+0.14	-35	+0.18	+0.12	+0.15	+1
Wet season	+0.20	+0.16	+0.18	-30	+0.20	+0.14	+0.17	+4
Dry season	+0.11	+0.12	+0.11	-2	+0.16	+0.12	+0.14	0

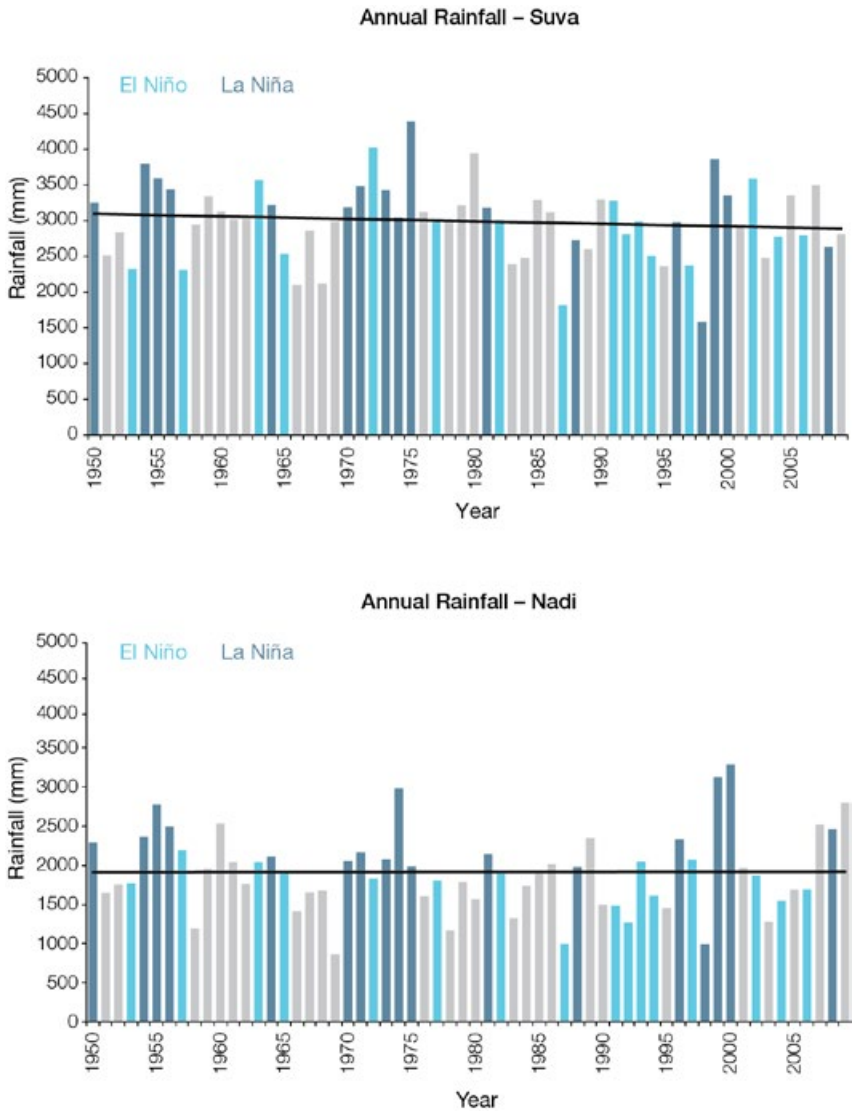

Figure 5.4: Annual rainfall for Suva (top) and Nadi Airport (bottom). Light blue, dark blue and grey bars denote El Niño, La Niña and neutral years respectively.

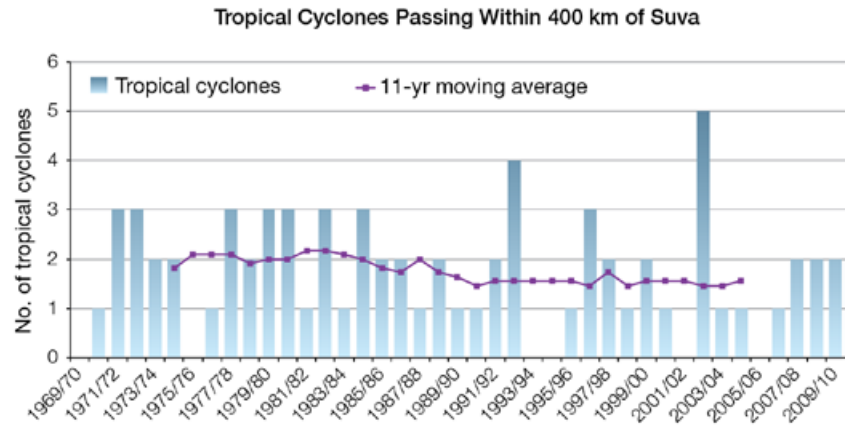

Figure 5.5: The number of tropical cyclones passing within 400 km of Suva per season. The 11-year moving average is in purple.

The neutral season average is 16 cyclones per decade. The interannual variability in the number of tropical cyclones in the vicinity of Suva is large, ranging from zero in some seasons to five in 2002/03. This variability makes it difficult to identify any long-term trends in frequency.

More than 80% of meteorological droughts since 1920 are associated with El Niño events. Severe droughts in recent times occurred in 1987, 1992, 1997/98, 2003 and 2010 (Figure 5.4). A special feature of Fiji droughts is a time lag of several months between the onset/end of moderate to strong El Niño events and the onset/end of droughts.

River flooding occurs almost every wet season and occasionally in the dry season during La Niña events. Most floods occur at the height of the wet season between January and March. Most rivers and streams in Fiji are relatively small and flow from steep mountainous terrain. The short and steep watercourses, together with high intensity rainfall, lead to swiftly rising and falling water levels. The time between rainfall and floods can be as short as a few hours, making prediction difficult.

Fires occasionally occur on the leeward sides of the main islands in the dry season during a significant period without rainfall. Other extreme events include storm surges and waves associated with significant tropical disturbances.

5.6.4 Sea-Surface Temperature

Historical changes in sea-surface temperature around Fiji are consistent with the broad-scale changes in the PCCSP region. Water temperatures remained relatively constant from the 1950s to the late 1980s. This was followed by a period of more rapid warming (approximately 0.07°C per decade for 1970–present). At these regional scales, natural variability plays a large role in changes to sea-surface temperature making it difficult to any identify long-term trends. Figure 5.8 shows the 1950–2000 sea-surface temperature changes (relative to a reference year of 1990) from three different large-scale sea-surface temperature gridded datasets (HadSST2, ERSST and Kaplan Extended SST V2; Volume 1, Table 2.3)

5.6.5 Ocean Acidification

Based the large-scale distribution of coral reefs across the Pacific and the seawater chemistry, Guinotte et al. (2003) suggested that seawater aragonite saturation states above 4 were optimal for coral growth and for the development of healthy reef ecosystems, with values from 3.5 to 4 adequate for coral growth, and values between 3 and 3.5, marginal. Coral reef ecosystems were not found at seawater aragonite saturation states below 3 and these conditions were classified as extremely marginal for supporting coral growth.

In the Fijian maritime boundaries, the aragonite saturation state has declined from about 4.5 in the late 18th century to an observed value of about 3.9 ± 0.1 by 2000.

5.6.6 Sea Level

Monthly averages of the historical tide gauge (both Suva and Lautoka), satellite (since 1993) and gridded sea-level (since 1950) data agree well after 1993 and indicate interannual variability in sea levels of about 18 cm (estimated 5–95% range) after removal of the seasonal cycle (Figure 5.10; Section 5.7.5). Prior to 1990, there are gaps in the Suva time series and changes in instrumentation may have led to data inhomogeneities. The sea-level rise near Fiji measured by satellite altimeters (Figure 5.6) since 1993 is about 6 mm per year, larger than the global average of 3.2 ± 0.4 mm per year. This rise is partly linked to a pattern related to climate variability from year to year and decade to decade (Figure 5.10).

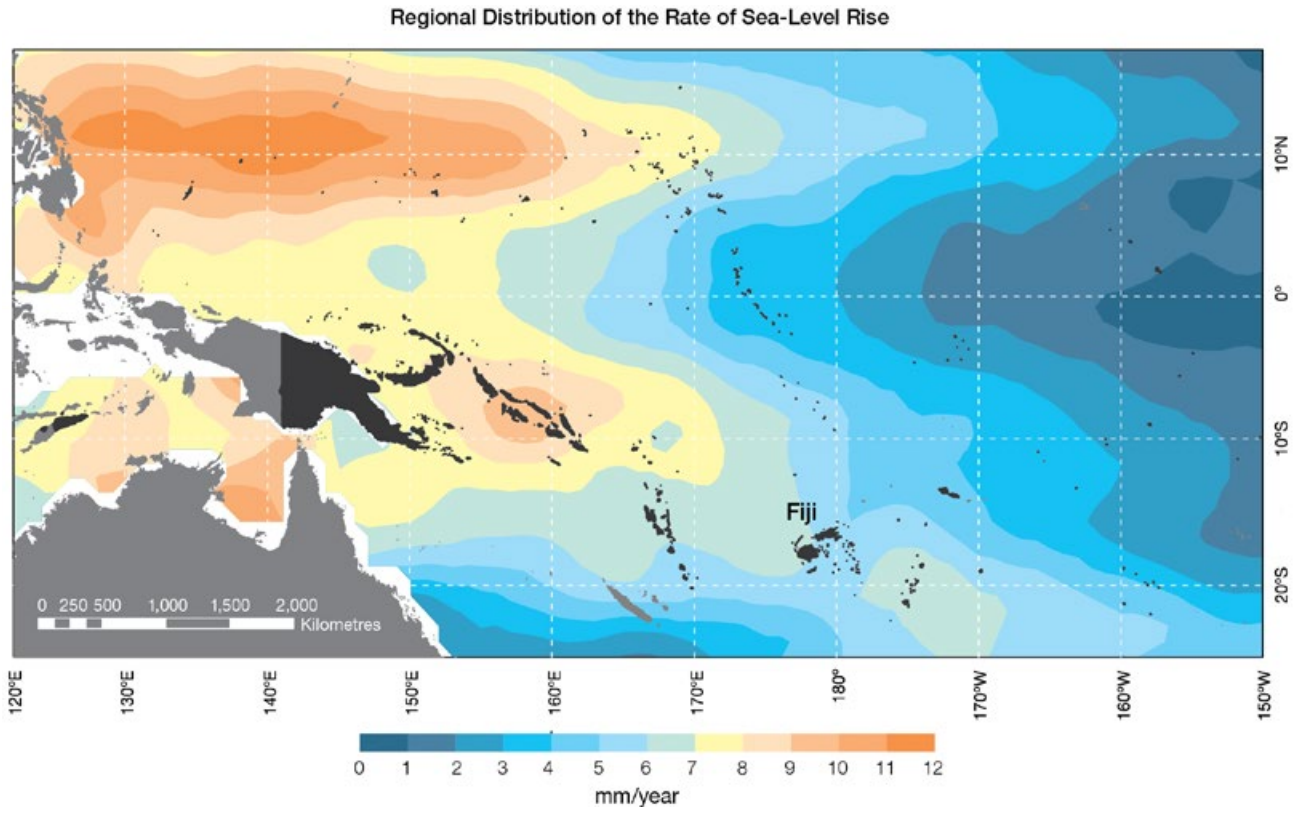

Figure 5.6: The regional distribution of the rate of sea-level rise measured by satellite altimeters from January 1993 to December 2010, with the location of Fiji indicated. Further detail about the regional distribution of sea-level rise is provided in Volume 1, Section 3.6.3.2.

5.6.7 Extreme Sea-Level Events

The annual climatology of the highest daily sea levels has been evaluated from hourly tide gauge measurements at Lautoka and Suva (Figure 5.7). Tidal variations throughout the year lead to highest annual water levels during November-March. Short-term contributions at Lautoka exhibit a weak annual cycle with higher levels during December-March. At Suva, the short-term contributions are higher in December-March as well as June and July which may be partly explained by Suva's south-east exposure to the stronger trade winds and waves at these times of the year. Although the average seasonal signal shows little variability throughout the year, there is a tendency for higher water levels at Suva and Lautoka from March through October during La Niña years whereas during El Niño years there is a tendency for lower seasonal sea levels during these months. The top 10 highest sea levels recorded at both sites mostly occur during the cyclone season. The highest recorded event at each site was associated with Tropical Cyclone Gavin in March 1997 while the second highest event at Lautoka in December 1992 was associated with Tropical Cyclone Joni. Other weather events contributing to the high water levels include tropical depressions and monsoon troughs.

Further research has been undertaken modelling storm surges from a large number of tropical cyclones with varying intensities, speeds and directions of approach, which fit the distributions of the cyclone parameters for cyclones that have affected Fiji in recent decades. This provides more detailed information on how extreme sea levels due to storm surges vary around the coastlines of Viti Levu and Vanua Levu. This modelling indicates that the north-western coastlines of both islands show the greatest risk of storm surges because they face the direction from which tropical cyclones most commonly approach Fiji. The 1-in-100-year storm surge heights along these coastlines were found to be around twice the values at locations situated on the south-west side of the islands (McInnes et al., 2011).

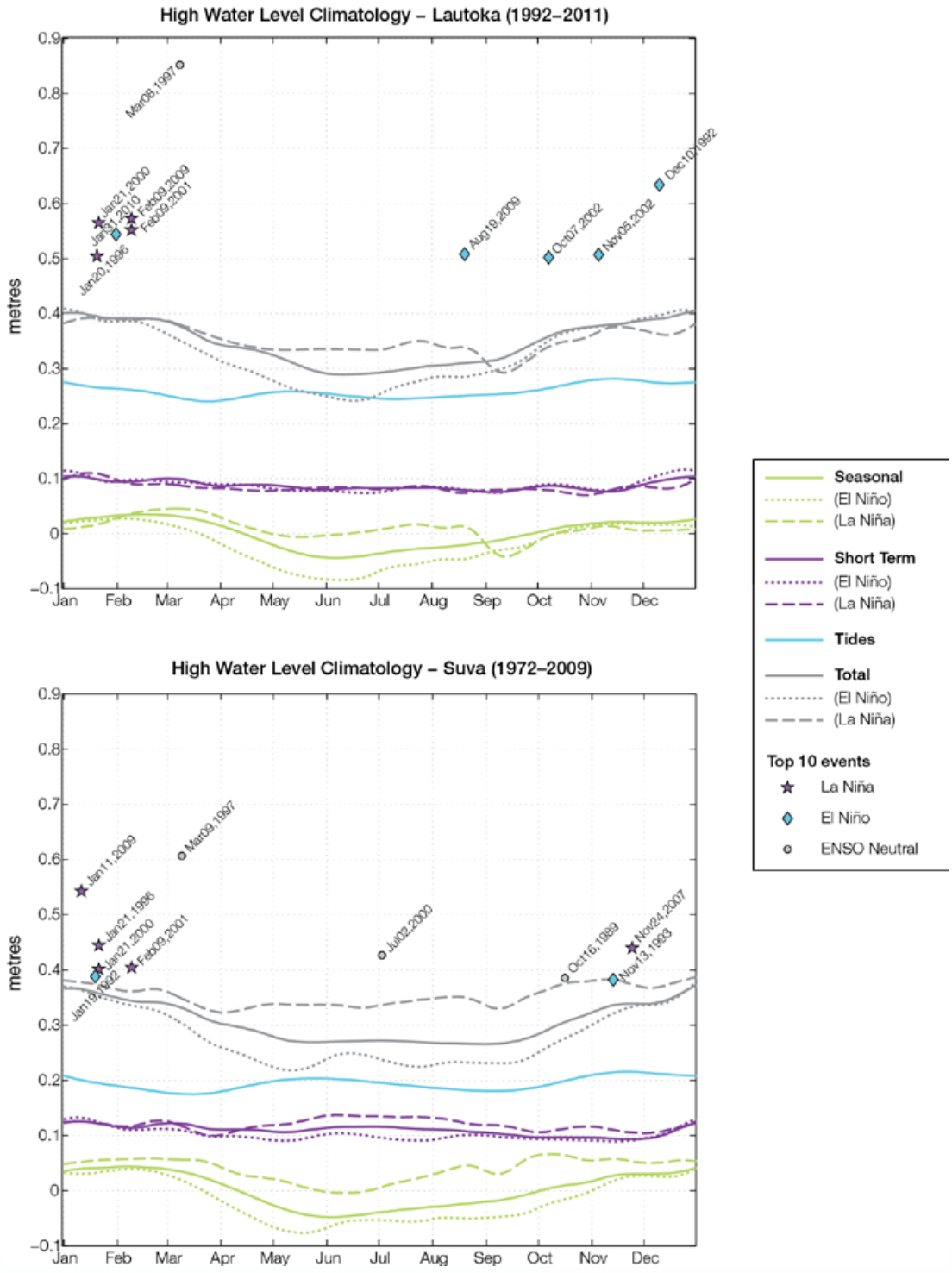

Figure 5.7: The annual cycle of high water relative to the Mean Higher High Water (MHHW) due to tides, short-term fluctuations (most likely associated with storms) and seasonal variations for Lautoka (top) and Suva (bottom). The tides and short-term fluctuations are respectively the 95% exceedence levels of the astronomical high tides relative to MHHW and the short-term sea-level fluctuations. Components computed only for El Niño and La Niña years are shown by dotted and dashed lines and grey lines are the sum of the tide, short-term and seasonal components. The 10 highest sea-level events in the record relative to MHHW are shown and coded to indicate the phase of ENSO at the time of the extreme event.

5.7 Climate Projections

Climate projections have been derived from up to 18 global climate models from the CMIP3 database, for up to three emissions scenarios (B1 (low), A1B (medium) and A2 (high)) and three 20-year periods (centred on 2030, 2055 and 2090, relative to 1990). These models were selected based on their ability to reproduce important features of the current climate (Volume 1, Section 5.2.3), so projections arising from each of the models are plausible representations of the future climate. This means there is not one single projected future for Fiji, but rather a range of possible futures. The full range of these futures is discussed in the following sections.

These projections do not represent a value specific to any actual location, such as a town or city in Fiji. Instead, they refer to an average change over the broad geographic region encompassing the islands of Fiji and the surrounding ocean (Figure 1.1 shows the regional boundaries). Some information regarding dynamical downscaling simulations from the CCAM model (Section 1.7.2) is also provided for temperature and rainfall projections, in order to indicate how changes in the climate on an individual island-scale may differ from the broad-scale average.

Section 1.7 provides important information about interpreting climate model projections.

5.7.1 Temperature

Surface air temperature and sea-surface temperature are projected to continue to increase over the course of the 21st century. There is *very high* confidence in this direction of change because:

- Warming is physically consistent with rising greenhouse gas concentrations.
- All CMIP3 models agree on this direction of change.

The majority of CMIP3 models simulate a slight increase (<1°C) in annual and seasonal mean temperature by 2030, however by 2090 under the A2 (high) emissions scenario temperature increases of greater than 2.5°C are simulated by the majority of models (Table 5.4). Given the close relationship between surface air temperature and sea-surface temperature, a similar (or slightly weaker) rate of warming is projected for the surface ocean (Figure 5.8). There is *moderate* confidence in this range and distribution of possible futures because:

- There is generally a large discrepancy between modelled and observed temperature trends over the past 50 years in the vicinity of Fiji (Figure 5.8).

The 8 km CCAM simulations suggest that warming may be stronger along the west coast of Viti Levu and Vanua Levu. These simulations also typically project an extra 0.5 to 1°C increase in temperature over land, relative to the change in surface air temperature over the ocean (Volume 1, Section 7.2.2.1).

Interannual variability in surface air temperature and sea-surface temperature over Fiji is strongly influenced by ENSO in the current climate (Section 5.5). As there is no consistency in projections of future ENSO activity (Volume 1, Section 6.4.1), it is not possible to determine whether interannual variability in temperature will change in the future. However, ENSO is expected to continue to be an important source of variability for Fiji.

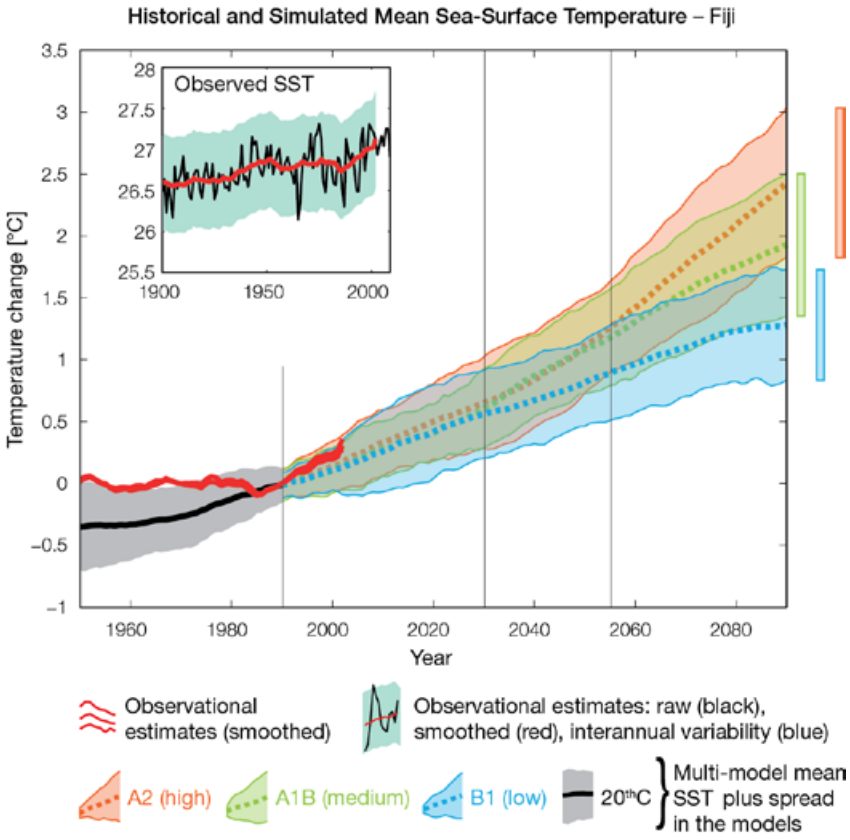

Figure 5.8: Historical climate (from 1950 onwards) and simulated historical and future climate for annual mean sea-surface temperature (SST) in the region surrounding Fiji, for the CMIP3 models. Shading represents approximately 95% of the range of model projections (twice the inter-model standard deviation), while the solid lines represent the smoothed (20-year running average) multi-model mean temperature. Projections are calculated relative to the 1980–1999 period (which is why there is a decline in the inter-model standard deviation around 1990). Observational estimates in the main figure (red lines) are derived from the HadSST2, ERSST and Kaplan Extended SST V2 datasets (Volume 1, Section 2.2.2). Annual average (black) and 20-year running average (red) HadSST2 data is also shown inset.

5.7.2 Rainfall

Wet Season (November-April)

Wet season rainfall is projected to increase over the course of the 21st century. There is *moderate* confidence in this direction of change because:

- An increase in wet season rainfall is consistent with the projected likely increase in the intensity of the South Pacific Convergence Zone (SPCZ), which lies over Fiji in this season (Volume 1, Section 6.4.5).
- The majority of CMIP3 models agree on this direction of change by 2090.

The majority of CMIP3 models simulate little change (-5% to 5%) in wet season rainfall by 2030, however by 2090 the majority simulate an increase (>5%), with approximately one third simulating a large increase (>15%) under the A2 (high) emissions scenario (Table 5.4). There is *moderate* confidence in this range and distribution of possible futures because:

- In simulations of the current climate, the CMIP3 models generally locate the SPCZ in the correct location relative to Fiji in the wet season (Brown et al., 2011).
- The CMIP3 models are unable to resolve many of the physical processes involved in producing rainfall. As a consequence, they do not simulate rainfall as well as other variables such as temperature (Volume 1, Chapter 5).

The 8 km CCAM simulations suggest that rainfall increases may be slightly higher than the large-scale CMIP3 projections along the eastern coastlines of Viti Levu and Vanua Levu. This is a physically plausible response for the windward side of mountainous islands (Volume 1, Section 7.2.2.1).

Dry Season (May-October)

Dry season rainfall is projected to decrease over the course of the 21st century. There is *moderate* confidence in this direction of change because:

- Approximately half of the CMIP3 models agree on this direction of change by 2090.

The majority of CMIP3 models simulate little change (-5% to 5%) in dry season rainfall by 2030, however by 2090 the models are approximately equally divided between a decrease (<-5%) and little change, with only two to three models suggesting an increase (>5%) depending on the emissions scenario (Table 5.4). There is *low* confidence in this range and distribution of possible futures because:

- In simulations of the current climate, some CMIP3 models have an SPCZ that extends too far east during the dry season, with too much rainfall over Fiji (Brown et al., 2011).
- The CMIP3 models are unable to resolve many of the physical processes involved in producing rainfall.

Annual

Little change is projected in total annual rainfall over the course of the 21st century. There is *low* confidence in this direction of change because:

- Only approximately half of the CMIP3 models agree on this direction of change by 2090.
- There is low confidence in the range and distribution of dry season rainfall projections, as discussed.

Interannual variability in rainfall over Fiji is strongly influenced by ENSO in the current climate, via the movement of the SPCZ (Section 5.5). As there is no consistency in projections of future ENSO activity (Volume 1, Section 6.4.1), it is not possible to determine whether interannual variability in rainfall will change in the future.

5.7.3 Extremes

Temperature

The intensity and frequency of days of extreme heat are projected to increase over the course of the 21st century. There is *very high* confidence in this direction of change because:

- An increase in the intensity and frequency of days of extreme heat is physically consistent with rising greenhouse gas concentrations.
- All CMIP3 models agree on the direction of change for both intensity and frequency.

The majority of CMIP3 models simulate an increase of approximately 1°C in the temperature experienced on the 1-in-20-year hot day by 2055 under the B1 (low) emissions scenario, with an increase of over 2.5°C simulated by the majority of models by 2090 under the A2 (high) emissions scenario (Table 5.4). There is *low* confidence in this range and distribution of possible futures because:

- In simulations of the current climate, the CMIP3 models tend to underestimate the intensity and frequency of days of extreme heat (Volume 1, Section 5.2.4).
- Smaller increases in the frequency of days of extreme heat are projected by the CCAM 60 km simulations.

Rainfall

The intensity and frequency of days of extreme rainfall are projected to increase over the course of the 21st century. There is *high* confidence in this direction of change because:

- An increase in the frequency and intensity of extreme rainfall is consistent with larger-scale projections, based on the physical argument that the atmosphere is able to hold more water vapour in a warmer climate (Allen and Ingram, 2002; IPCC, 2007). It is also consistent with the projected likely increase in SPCZ intensity (Volume 1, Section 6.4.5).
- Almost all of the CMIP3 models agree on this direction of change for both intensity and frequency.

The majority of CMIP3 models simulate an increase of at least 10 mm in the amount of rain received on the 1-in-20-year wet day by 2055 under the B1 (low) emissions scenario, with an increase of at least 25 mm simulated by 2090 under the A2 (high) emissions scenario. The majority of models project that the current 1-in-20-year extreme rainfall event will occur, on average, three times

per 20-year period by 2055 under the B1 (low) emissions scenario and four to five times per 20-year period by 2090 under the A2 (high) emissions scenario. There is *low* confidence in this range and distribution of possible futures because:

- In simulations of the current climate, the CMIP3 models tend to underestimate the intensity and frequency of extreme rainfall (Volume 1, Section 5.2.4).
- The CMIP3 models are unable to resolve many of the physical processes involved in producing extreme rainfall.

Drought

Little change is projected in the incidence of drought over the course of the 21st century. There is *low* confidence in this direction of change because:

- There is only low confidence in the range of dry season rainfall projections (Section 5.7.2), which directly influences projections of future drought conditions.

Under the B1 (low) emissions scenario, the majority of CMIP3 models project that the frequency of mild drought will slightly increase from approximately seven to eight times every 20 years in 2030, to eight to nine times every 20 years by 2090. Under the A1B (medium) emissions scenario, the frequency of mild drought remains approximately constant at seven to eight times every 20 years, while under the A2 (high) emissions scenario the frequency is projected to slightly decrease from eight to nine times every 20 years in 2030 to seven to eight times by 2090. The majority of CMIP3 models project that moderate and severe droughts will occur approximately once to twice and once every 20 years respectively, across all time periods and emissions scenarios.

Tropical Cyclones

Tropical cyclone numbers are projected to decline in the south-east Pacific Ocean basin (0–40ºS, 170ºE–130ºW) over the course of the 21st century. There is *moderate* confidence in this direction of change because:

- Many studies suggest a decline in tropical cyclone frequency globally (Knutson et al., 2010).
- Tropical cyclone numbers decline in the south-east Pacific Ocean in the majority assessment techniques.

Based on the direct detection methodologies (Curvature Vorticity Parameter (CVP) and the CSIRO Direct Detection Scheme (CDD) described in Volume 1, Section 4.8.2), 65% of projections show no change or a decrease in tropical cyclone formation when applied to the CMIP3 climate models for which suitable output is available. When these techniques are applied to CCAM, 100% of projections show a decrease in tropical cyclone formation. In addition, the Genesis Potential Index (GPI) empirical technique suggests that conditions for tropical cyclone formation will become less favourable in the south-east Pacific Ocean basin for all analysed CMIP3 models. There is *moderate* confidence in this range and distribution of possible futures because in simulations of the current climate, the CVP, CDD and GPI methods capture the frequency of tropical cyclone activity reasonably well (Volume 1, Section 5.4).

Despite this projected reduction in total cyclone numbers, five of the six CCAM 60 km simulations show an increase in the proportion of the most severe cyclones. Most models also indicate a reduction in tropical cyclone wind hazard north of 20ºS latitude and regions of increased hazard south of 20ºS latitude. This increase in wind hazard coincides with a poleward shift in the latitude at which tropical cyclones are most intense.

5.7.4 Ocean Acidification

The acidification of the ocean will continue to increase over the course of the 21st century. There is *very high* confidence in this projection as the rate of ocean acidification is driven primarily by the increasing oceanic uptake of carbon dioxide, in response to rising atmospheric carbon dioxide concentrations.

Projections from all analysed CMIP3 models indicate that the annual maximum aragonite saturation state will reach values below 3.5 by about 2035 and continue to decline thereafter (Figure 5.9; Table 5.4). There is *moderate* confidence in this range and distribution of possible futures because the projections are based on climate models without an explicit representation of the carbon cycle and with relatively low resolution and known regional biases.

The impact of acidification change on the health of reef ecosystems is likely to be compounded by other stressors including coral bleaching, storm damage and fishing pressure.

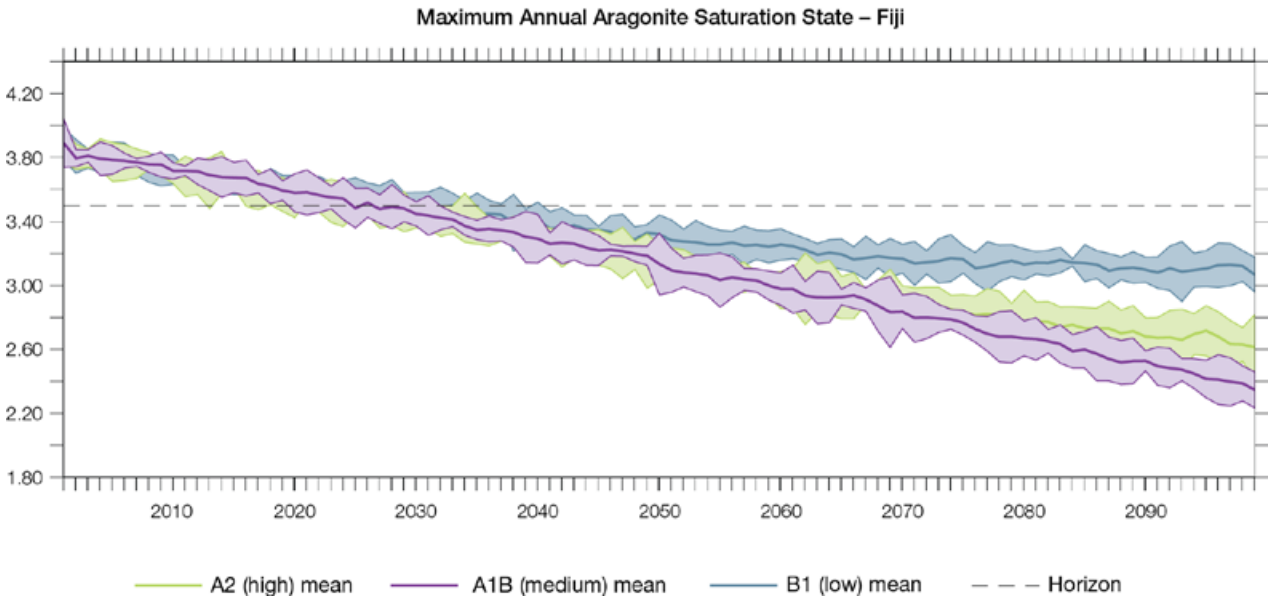

Figure 5.9: Multi-model projections, and their associated uncertainty (shaded area represents two standard deviations), of the maximum annual aragonite saturation state in the sea surface waters of the Fiji region under the different emissions scenarios. The dashed black line represents an aragonite saturation state of 3.5.

5.7.5 Sea Level

Mean sea level is projected to continue to rise over the course of the 21st century. There is *very high* confidence in this direction of change because:

- Sea-level rise is a physically consistent response to increasing ocean and atmospheric temperatures, due to thermal expansion of the water and the melting of glaciers and ice caps.
- Projections arising from all CMIP3 models agree on this direction of change.

The CMIP3 models simulate a rise of between approximately 5–15 cm by 2030, with increases of 20–60 cm indicated by 2090 under the higher emissions scenarios (i.e. A2 (high) and A1B (medium); Figure 5.10; Table 5.4). There is *moderate* confidence in this range and distribution of possible futures because:

- There is significant uncertainty surrounding ice-sheet contributions to sea-level rise and a larger rise than that projected above cannot be excluded (Meehl et al., 2007b). However, understanding of the processes is currently too limited to provide a best estimate or an upper bound (IPCC, 2007).
- Globally, since the early 1990s, sea level has been rising near the upper end of the these projections. During the 21st century, some studies (using semi-empirical models) project faster rates of sea-level rise.

Interannual variability of sea level will lead to periods of lower and higher regional sea levels. In the past, this interannual variability has been about 18 cm (5–95% range, after removal of the seasonal cycle; dashed lines in Figure 5.10 (a)) and a similar range is likely to continue through the 21st century. In addition, winds and waves associated with weather phenomena will continue to lead to extreme sea-level events.

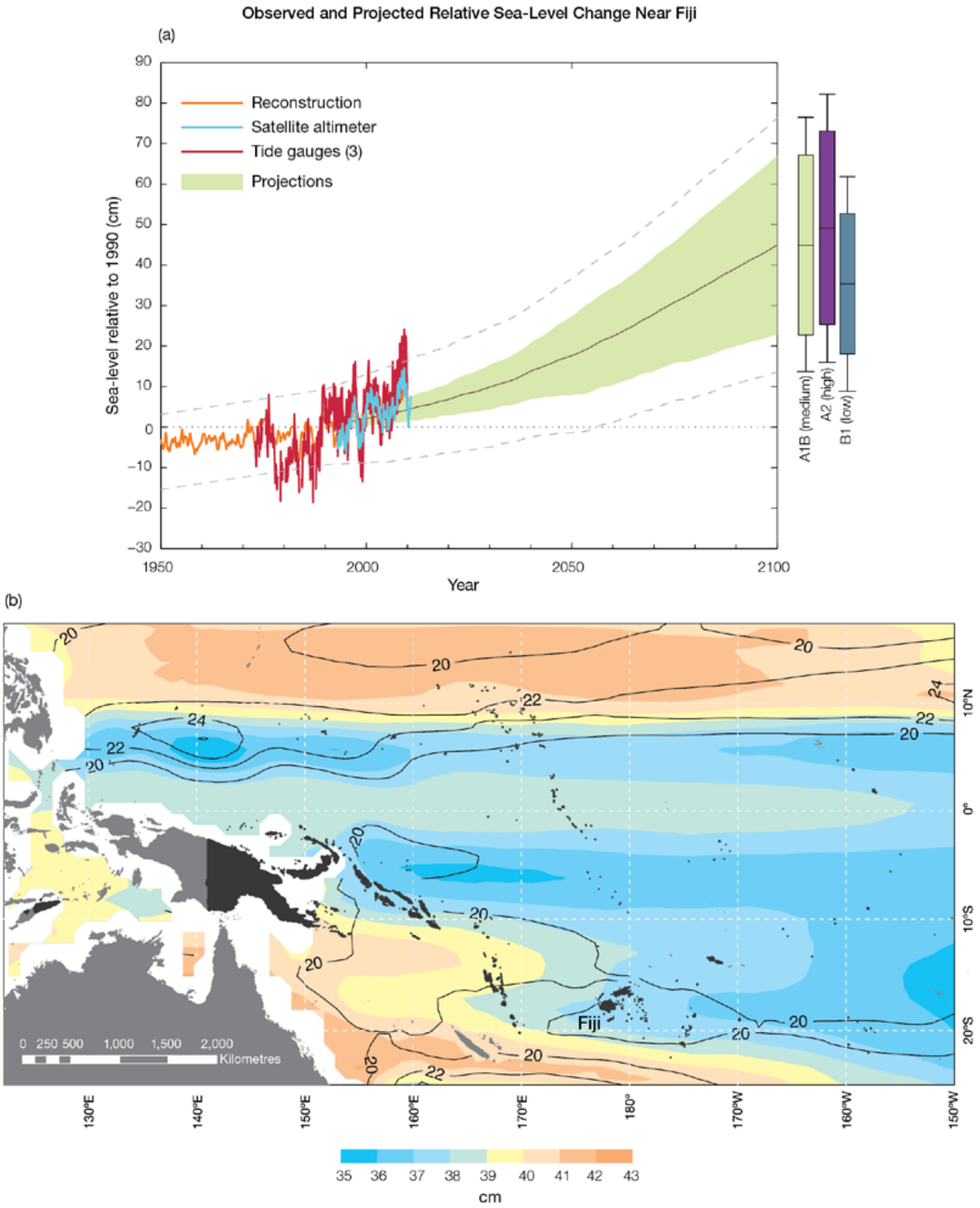

Figure 5.10: Observed and projected relative sea-level change near Fiji. (a) The observed in situ relative sea-level records from Suva (since the early 1970s) and Lautoka (since 1992) are indicated in red, with the satellite record (since 1993) in light blue. The gridded sea-level data at Fiji (since 1950, from Church and White (in press)) is shown in orange. The projections for the A1B (medium) emissions scenario (5–95% uncertainty range) are shown by the green shaded region from 1990–2100. The range of projections for the B1 (low), A1B (medium) and A2 (high) emissions scenarios by 2100 are also shown by the bars on the right. The dashed lines are an estimate of interannual variability in sea level (5–95% range about the long-term trends) and indicate that individual monthly averages of sea level can be above or below longer-term averages. (b) The projections (in cm) for the A1B (medium) emissions scenario in the Fiji region for the average over 2081–2100 relative to 1981–2000 are indicated by the shading, with the estimated uncertainty in the projections indicated by the contours (in cm).

5.7.6 Projections Summary

The projections presented in Section 5.7 are summarised in Table 5.4. For detailed information regarding the various uncertainties associated with the table values, refer to the preceding text in Sections 5.7 and 1.7, in addition to Chapters 5 and 6 in Volume 1. When interpreting the differences between projections for the B1 (low), A1B (medium) and A2 (high) emissions scenarios, it is also important to consider the emissions pathways associated with each scenario (Volume 1, Figure 4.1) and the fact that a slightly different subset of models was available for each (Volume 1, Appendix 1).

Table 5.4: Projected change in the annual and seasonal mean climate for Fiji, under the B1 (low; blue), A1B (medium; green) and A2 (high; purple) emissions scenarios. Projections are given for three 20-year periods centred on 2030 (2020–2039), 2055 (2046–2065) and 2090 (2080–2099), relative to 1990 (1980–1999). Values represent the multi-model mean change ± twice the inter-model standard deviation (representing approximately 95% of the range of model projections), except for sea level where the estimated mean change and the 5–95% range are given (as they are derived directly from the Intergovernmental Panel on Climate Change Fourth Assessment Report values). The confidence (Section 1.7.2) associated with the range and distribution of the projections is also given (indicated by the standard deviation and multi-model mean, respectively). See Volume 1, Appendix 1 for a complete listing of CMIP3 models used to derive these projections.

Variable	Season	2030	2055	2090	Confidence
Surface air temperature (°C)	Annual	+0.6 ± 0.4 +0.7 ± 0.5 +0.7 ± 0.3	+1.0 ± 0.5 +1.4 ± 0.5 +1.4 ± 0.3	+1.4 ± 0.7 +2.1 ± 0.8 +2.6 ± 0.6	Moderate
Maximum temperature (°C)	1-in-20-year event	N/A	+1.0 ± 0.7 +1.4 ± 0.7 +1.5 ± 0.6	+1.3 ± 0.5 +2.1 ± 0.9 +2.6 ± 1.4	Low
Minimum temperature (°C)	1-in-20-year event	N/A	+1.1 ± 1.7 +1.5 ± 1.8 +1.5 ± 1.8	+1.5 ± 1.8 +1.9 ± 2.1 +2.3 ± 1.8	Low
Total rainfall (%)*	Annual	+3 ± 11 +1 ± 12 +2 ± 13	+1 ± 10 +3 ± 14 +4 ± 13	+2 ± 14 +3 ± 16 +7 ± 15	Low
Wet season rainfall (%)*	November-April	+5 ± 10 +3 ± 11 +5 ± 14	+5 ± 12 +6 ± 16 +7 ± 13	+5 ± 18 +8 ± 19 +14 ± 14	Moderate
Dry season rainfall (%)*	May-October	-1 ± 13 -2 ± 17 -2 ± 12	-5 ± 14 -2 ± 16 -1 ± 18	-3 ± 17 -4 ± 19 -1 ± 22	Low
Sea-surface temperature (°C)	Annual	+0.6 ± 0.4 +0.6 ± 0.3 +0.7 ± 0.4	+0.9 ± 0.4 +1.2 ± 0.4 +1.3 ± 0.4	+1.3 ± 0.4 +1.9 ± 0.6 +2.4 ± 0.4	Moderate
Aragonite saturation state (Ωar)	Annual maximum	+3.5 ± 0.1 +3.4 ± 0.1 +3.4 ± 0.1	+3.2 ± 0.1 +3.0 ± 0.1 +3.0 ± 0.1	+3.1 ± 0.1 +2.6 ± 0.1 +2.5 ± 0.1	Moderate
Mean sea level (cm)	Annual	+10 (5–16) +10 (5–15) +10 (3–16)	+18 (10–27) +20 (9–31) +20 (8–31)	+32 (16–47) +39 (20–59) +41 (21–62)	Moderate

*The MIROC3.2(medres) and MIROC3.2(hires) models were eliminated in calculating the rainfall projections, due to their inability to accurately simulate present-day activity of the South Pacific Convergence Zone (Volume 1, Section 5.5.1).